International Journal of Astrobiology 5 (2): 151–169 (2006) Printed in the United Kingdom
doi:10.1017/S1473550406003053 First published online 19 September 2006

Effects of artificial lighting on the detection of plant stress with spectral reflectance remote sensing in bioregenerative life support systems

Andrew C. Schuerger[1] and Jeffrey T. Richards[2]

[1]*Department of Plant Pathology, University of Florida, Building M6-1025, Space Life Sciences Lab, Kennedy Space Center, FL 32899, USA*
e-mail: acschuerger@ifas.ufl.edu
[2]*Dynamac Corporation, Building M6-1025, Space Life Sciences Lab, Kennedy Space Center, FL 32899, USA*

Abstract: Plant-based life support systems that utilize bioregenerative technologies have been proposed for long-term human missions to both the Moon and Mars. Bioregenerative life support systems will utilize higher plants to regenerate oxygen, water, and edible biomass for crews, and are likely to significantly lower the 'equivalent system mass' of crewed vehicles. As part of an ongoing effort to begin the development of an automatic remote sensing system to monitor plant health in bioregenerative life support modules, we tested the efficacy of seven artificial illumination sources on the remote detection of plant stresses. A cohort of pepper plants (*Capsicum annuum* L.) were grown 42 days at 25 °C, 70% relative humidity, and 300 μmol m^{-2} s^{-1} of photosynthetically active radiation (PAR; from 400 to 700 nm). Plants were grown under nutritional stresses induced by irrigating subsets of the plants with 100, 50, 25, or 10% of a standard nutrient solution. Reflectance spectra of the healthy and stressed plants were collected under seven artificial lamps including two tungsten halogen lamps, plus high pressure sodium, metal halide, fluorescent, microwave, and red/blue light emitting diode (LED) sources. Results indicated that several common algorithms used to estimate biomass and leaf chlorophyll content were effective in predicting plant stress under all seven illumination sources. However, the two types of tungsten halogen lamps and the microwave illumination source yielded linear models with the highest residuals and thus the highest predictive capabilities of all lamps tested. The illumination sources with the least predictive capabilities were the red/blue LEDs and fluorescent lamps. Although the red/blue LEDs yielded the lowest residuals for linear models derived from the remote sensing data, the LED arrays used in these experiments were optimized for plant productivity and not the collection of remote sensing data. Thus, we propose that if adjusted to optimize the collection of remote sensing information from plants, LEDs remain the best candidates for illumination sources for monitoring plant stresses in bioregenerative life support systems.

Received 2 February 2006, accepted 7 July 2006

Key words: CELSS, ALS, bioregenerative life support system, plant stress, remote sensing.

Introduction

Plants are likely to be an integral part of any Advanced Life Support (ALS) system for future long-term human missions to the Moon or Mars because bioregenerative ALS technologies are the only processes that can partially or completely close the life support loops in crewed spacecraft (Olson *et al*. 1988; Ming & Henninger 1989; Schwartzkopf 1992; Wheeler *et al*. 2003). Bioregenerative ALS systems will utilize higher plants, such as beans, lettuce, potato, and wheat (Tibbits & Alford 1982; Wheeler *et al*. 2003) to recycle water, oxygen, and edible biomass during long-term missions to the Moon or Mars. Early modelling on what is called the 'equivalent system mass' (ESM) of a life support system indicates that after a 1–2 year period, the ESM of a bioregenerative ALS system is likely to be lower than the ESM of a non-bioregenerative ALS system (Drysdale *et al*. 1999; Eckart 1996; Ewert *et al*. 2001). The term ESM is defined as the total sum of all components of an ALS system that must be considered when comparing the total launched mass of a system and includes at least the following factors: direct launched mass, energy requirements of all subsystems, personnel time required for maintenance and repair, and operational constraints dictated by the systems (Drysdale *et al*. 1999; Ewert *et al*. 2001). However, the exact nature and complexity of a Mars bioregenerative ALS system has not yet been described.

A diversity of plant growing systems have been proposed and tested for bioregenerative systems including aeroponic,

hydroponic, membrane-hydration, *in situ* regolith, and zeolite plant support systems (see Olson *et al.* (1988); Ming & Henninger (1989); Schwartzkopf (1992); Wheeler *et al.* (2003) and the citations within these reports). In addition, a wide range of illumination systems have been suggested for the primary production of edible biomass including natural *in situ* solar radiation on Mars (Olson *et al.* 1988; Wheeler & Martin-Brennan 2000) and artificial illumination sources including high-pressure sodium (HPS), metal halide (MH), fluorescent (FL), microwave (MCW), and light-emitting diode (LED) lamps (Bula *et al.* 1991; Barta *et al.* 1992; Brown *et al.* 1995; Goins *et al.* 1997; Schuerger & Brown 1997; Goins and Yorio 2000; Wheeler & Martin-Brennan 2000; Wheeler *et al.* 2003; Kim *et al.* 2004a). LED arrays have gained significant attention in recent years because they are extremely long-lived, have small heat signatures, consume low levels of energy, and are considered to be one of the safest artificial light sources for plant production in space habitats (Bula *et al.* 1991; Goins *et al.* 1997; Goins & Yorio 2000; Kim *et al.* 2004a, b).

Several papers have appeared in the literature that discuss potential microbial issues in ALS systems that cover the range of problems from the formation of biofilms that interfere with nominal operations of ALS components to plant–pathogen interactions leading to significant impairment of crop productivity (Gonzales *et al.* 1996; Schuerger 1998, 2004; Schuerger *et al.* 2002). Furthermore, several recent studies have proposed the use of remote sensing technologies to monitor plant health in bioregenerative ALS systems, including spectral reflectance, leaf fluorescence, and thermal imaging (Woodhouse *et al.* 1994; Omasa 2001; Norikane *et al.* 2003; Paul *et al.* 2004). However, no papers were found in the literature that explored the effects of artificial lighting in ALS systems on typical remote sensing algorithms such as infrared-to-red band ratios and the Normalized Difference Vegetation Index (NDVI) (see Lillesand & Kiefer (1994); Lichtenthaler (1996); Schowengerdt (1997)).

The primary objective of the current study was to compare several artificial illumination sources in a side-by-side comparison with a single cohort of stressed plants to determine the efficacy of each illumination source in detecting plant stress under simulated ALS conditions. Seven lamps were used in these experiments including two types of tungsten halogen lamps, plus HPS, MH, fluorescent, MCW, and LED sources. These artificial illumination sources were selected based on previous studies with these lamps on crop productivity for ALS systems (Bula *et al.* 1991; Barta *et al.* 1992; Brown *et al.* 1995; Goins *et al.* 1997; Schuerger & Brown 1997; Goins & Yorio 2000; Kim *et al.* 2004a, b). These experiments were part of an ongoing effort to design an automatic bio-monitoring system for use within ALS modules to detect plant stress. The primary goal for developing such an automatic remote sensing system for plant monitoring is to reduce the ESM of bioregenerative ALS systems. An automatic remote monitoring system could reduce the launched mass and long-term energy consumption of an ALS system, plus minimize crew-time required for scouting the plant production modules for deviations from normal operations. A second application of such an automatic bio-monitoring system would be in the deployment of a plant biology experiment to the Martian surface to test the biotoxicity of the Martian regolith (Ferl *et al.* 2002; Paul *et al.* 2004).

Materials and methods

Plant production

Seeds of 'Hungarian Wax' pepper (*Capsicum annuum* L.) were planted in 20–30 mesh silica sand in autoclavable plastic containers (GA-7 Magenta Vessels, Sigma-Aldrich Chemical, Co., St. Louis, MO, USA). The sand/plastic container units were previously sterilized by autoclaving at 121 °C and 1.1 kg cm^{-2} for 1 h. Seeds were irrigated with a complete nutrient solution (NS) (Schuerger & Mitchell 1992) composed of reagent grade salts (all from Sigma-Aldrich) that yielded final concentrations (reported as mg l^{-1}) for the following ions: nitrogen (175), phosphorous (30), potassium (160, calcium (225), magnesium (45), sulphur (72), boron (0.35), iron (5), copper (0.2), manganese (0.8), and molybdenum (0.005). All NSs were adjusted to pH 5.5 prior to use. The electrical conductivity of the full-strength NS was 1.7 S m^{-1}.

Magenta Vessels with germinating seeds were placed into a plant growth chamber (model M-15, Environmental Growth Chambers, Chagrin Falls, OH, USA) at 25 °C, 75% relative humidity, 300 μmol m^{-2} s^{-1} PAR, and a diurnal light regime of 16 h day and 8 h night. The seedlings were covered with polypropylene tops to promote seed germination. After 7 days, the tops were removed, and the germinating seedlings irrigated with 100, 50, 25, or 10% of full-strength NS for the duration of the experiments. In preliminary experiments with peppers, these NS concentrations were found to induce uniform symptoms in the 50, 25, and 10% nutrient levels that produced chlorotic and stunted plants increasing in severity from 50 to 10% nutrient concentrations (Fig. 1(d)).

Plants were grown for 42 days from seeding and then measured for spectral reflectance under each lamp. After completing all spectral measurements, plants were destructively harvested for the following: plant height (cm), total chlorophyll (reported as μg cm^{-2} of leaf area), number of leaves, leaf fresh weight (g), and leaf area (cm^2). Chlorophyll concentrations were estimated by measuring leaf absorption of infrared light by a hand-held SPAD-502 chlorophyll meter (Minolta, CO., Ltd., Japan), and then converting the SPAD-values to total chlorophyll concentrations by the following formulae:

$$y = 0.98(x) - 5.4 \quad [1]$$

in which y equals the total chlorophyll concentration in leaves (in μg cm^{-2}), x equals the SPAD value obtained for each plant, and the Residual (r^2) equaled 0.926 for the linear regression model (Schuerger unpublished model).

Plants were grown only under the cool-white FL lamps used in the M-15 growth chambers, and then transferred to a

https://doi.org/10.1017/S1473550406003053 Published online by Cambridge University Press

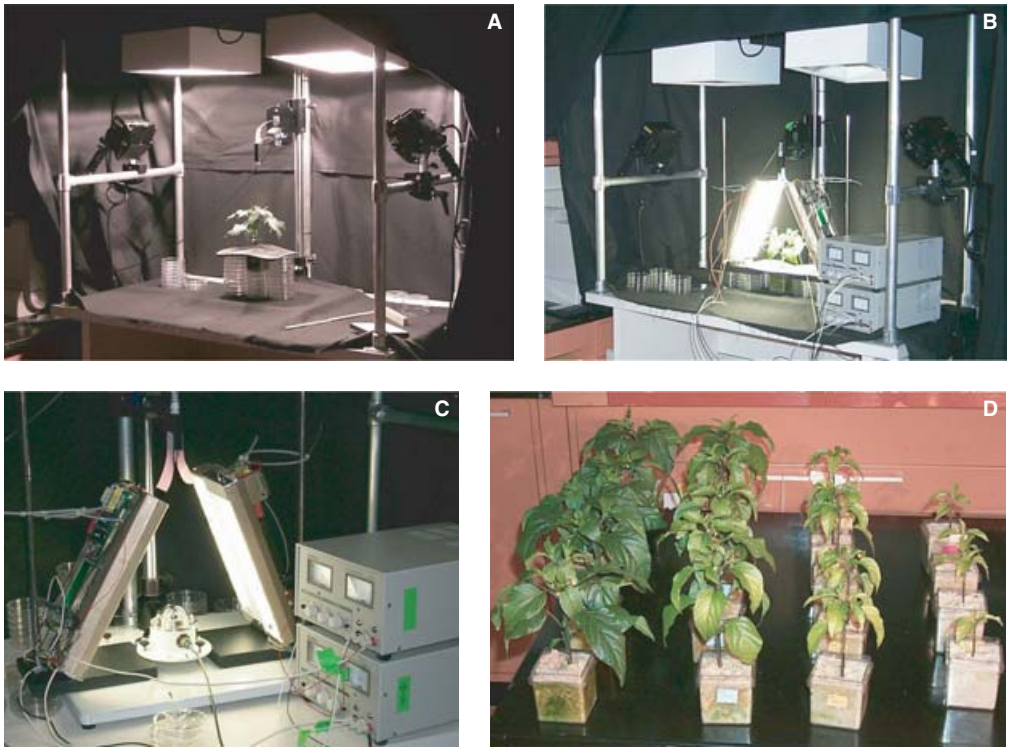

Fig. 1. Experimental setup for spectral reflectance measurements under seven artificial light sources. (A) Tungsten-halogen lamps (3200K) were mounted on side-bars of the aluminium scaffold, MH, HPS, and MCW lamps were mounted on the top of the scaffold, and plants placed on the black cloth centred under the lighting sources. (B) FL and LED lamps were placed in close proximity to the plant canopies. (C) The Eppley PSP pyranometer (800–3000 nm) and Eppley PIR pyrgeometer (3000–50 000 nm) sensors were placed at the same visible light intensity (300 μmol m^{-2} s^{-1} PAR) under each lamp as were the plant canopies. (D) Pepper (*Capsicum annuum* L.) plants were grown at 100, 50, 25, or 10% nutrient levels (from left to right).

separate lab in which all of the spectral reflectance measurements were made under the different illuminations sources. This was required to grow a cohort of plants under a single 'standard' illumination source so that any measured differences would be due to the illumination sources used for remote sensing measurements and not due to growth conditions.

Artificial light sources

Seven artificial light sources were used to illuminate plant canopies for both energy measurements and collection of reflectance spectra. (1) Two, 450 W tungsten-halogen lamps (model Lowell Omni-Light, Lowell-Light Manufacturing, Inc. Brooklyn, NY, USA) rated for a colour temperature of 3200°K (henceforth 3200K) were used as the control light source. (2) In order to alter the colour temperature of the tungsten 3200K lamps to a daylight balance, dichroic filters were used to convert the 3200K illumination to 5600°K light (henceforth 5600K). Thus, both the 3200K and 5600K data presented below used the same model of tungsten-halogen lamps, but the 5600K data used the dichroic filter to alter the colour temperature of the visible light. (3) Two, 400 W MH lamps were obtained from Energy Technics, York, PA, USA (model ETAC-400-MH-CH). (4) Two, 400 W high-pressure sodium (HPS) lamps were also obtained from Energy Technics (model ETAC-400-HPS). (5) One, 1000 W MCW lamp was obtained from Fusion Lighting, Rockville, MD, USA (model 1000 W-M). (6) Two, 30 W direct current (DC) FL lamps were constructed in-house using off-the-shelf electronic components. Each FL lamp measured 30 cm in length and 15 cm in width, and was powered by a 20 A DC voltage regulator (model GP-305, LG Precision, CO., Ltd., Melrose, MA, USA). (7) Two LED arrays were obtained from Quantum Devices, Inc., Barneveld, WI, USA (model Snap-Lite) and were composed of 2/3 red LEDs at a peak spectral output of 660 nm and 1/3 blue LEDs at peak spectral output of 460 nm. The LED arrays were powered by DC-voltage regulators supplied by Quantum Devices. Each LED array measured 15 × 15 cm.

The seven artificial illumination sources were configured in three basic ways for these experiments (Fig. 1). First, the tungsten 3200K lamps were placed on an aluminium scaffold at 45 deg off-nadir positions and approximately 0.75 m from plant canopies or spectroradiometers (Fig. 1(a)). The dichroic filters used to adjust the 3200K light to a colour temperature of 5600K were attached to the barn-door shields mounted on the front of the 3200K lamps. Thus, the dichroic filters could be easily swung into and out of place as required. Second, the MH, HPS, and MCW lamps were suspended from the top of the aluminium scaffold at 20 deg off-nadir positions and approximately 0.75 m from plant canopies or spectroradiometers (Figs 1(a) and 1(b)). The FL and LED

https://doi.org/10.1017/S1473550406003053 Published online by Cambridge University Press

lamps were placed on metal ring stands and configured very close to plant canopies or spectroradiometers (Figs 1(b) and 1(c)).

It was critical to align the seven lamps to deliver nearly identical levels of photosynthetically active radiation (PAR; 400–700 nm) to the tops of plant canopies or irradiation detectors. By doing so, the energy measurements and remote sensing data could be collected under lighting conditions similar to those found in the plant growth chambers used to produce the healthy and diseased plant canopies. Thus, each lamp type was precisely adjusted to deliver uniform illumination that measured 300 μmol m^{-2} s^{-1} of PAR as measured with a hand-held light meter (model LI-189, LI-COR, Inc., Lincoln, NE, USA). Although each lamp type emitted different levels of ultraviolet (UV), visible (VIS), near-infrared (NIR), and thermal infrared (ThIR) radiation (Fig. 2 and Table 1), the lamps were all adjusted to a similar PAR of 300 μmol m^{-2} s^{-1} of VIS light, and, thus, were measured under a common illumination level in order to standardize the light environment for these experiments.

Energy measurements of artificial lights

Spectral scans from 300 to 1100 nm were collected for each lamp with a spectroradiometer (model LI-1800, LI-COR, Inc.) under equal PAR densities of 300 μmol m^{-2} s^{-1}. Energy and photon flux densities were derived from these data. Radiation measurements from 800 to 3000 nm (near-infrared) were made with a PSP pyranometer (The Eppley Laboratory, Newport, RI, USA) with a Schott cut-on filter at 805 nm. Radiation from 3000 to 50 000 nm (thermal infrared) was measured with an Eppley PIR pyrgeometer with a silicon cut-on filter at 3000 nm.

In order to monitor the energy output of the lamps over short periods of time, the total light output of each lamp was measured with a 0.5×0.2 m solar panel connected to a DC-voltage oscilloscope (model TDS-784D, Tectronic, Inc. Wilsonville, OR, USA). The oscilloscope was capable of recording the energy fluctuations in the output of each lamp down to the millisecond level. The solar panel was placed below the seven lamps at different distances but at identical PAR levels of 300 μmol m^{-2} s^{-1}.

Spectral measurements of plant canopies illuminated with seven different light sources

Spectral reflectance measurements of plant canopies were made under each lamp with an Analytical Spectral Devices (ASD) Field-Spec Pro spectroradiometer (from ASD, Boulder, CO, USA). The Field-Spec Pro system was capable of measuring spectral reflectance from 350 to 2500 nm in 1 nm bands. All reflectance spectra were generated relative to a 99% reflectance panel (model SRT-99-050, Labsphere, Inc., North Sutton, NH, USA). The ASD spectroradiometer detector was mounted on a solid camera stand and placed in the centre of the illuminated area under the aluminium scaffold that held the various lamps (Fig. 1). A 25 deg field-of-view (FOV) fibre-optic sensor was used for all measurements. The 25 deg FOV sensor was maintained at 25 cm above plant canopies, regardless of the canopy size or structure. Magenta vessels that held the pepper plants were marked on one side in order to always align the plant canopies to face forward for spectral measurements. Thus, all plants were measured under the seven lamps with their canopies aligned to face in the same direction. This decreased the effects of canopy structure and leaf angles among the spectral measurements. In addition, a line-voltage regulator (model AR-1215, Furman Sound, Inc., Petaluma, CA, USA) was used to condition the line voltage of incoming power for the alternating current (AC) lamps (i.e. 3200K, 5600K, MH, HPS, and MCW lamps).

Plants were placed one at a time in the centre of the aluminium scaffolding and a reflectance spectrum collected for 25 averaged scans by the ASD Field-Spec Pro spectroradiometer (Fig. 1(a)). The aluminium scaffolding had been previously covered by a black cotton cloth to reduce stray light from the various lamps. All measurements were made with only the illumination source being tested turned-on; all room lights were turned-off. The configuration for the tungsten 3200K, tungsten 5600K, MH, HPS, and MCW lamps is given in Fig. 1(a). The FL and LED lamps had much lower light output than the other lamps and thus had to be placed in close proximity to the plant canopies (Fig. 1(b)). Care was taken to shield the 25 deg FOV sensor of the ASD spectroradiometer from specular reflections from the FL and LED lamps. All plants were measured in the same sequence for all lamps, and all plant measurements for a given lamp were collected at one time. However, the ASD spectroradiometer collects reflectance spectra very quickly and thus only 20 mins were required to measure all plants for a given lamp. Once spectral reflectance measurements for all lamps were completed the plants were destructively harvested for biometric data, as discussed above.

Reflectance (R) values at three individual spectral bands (R550, R685, and R760) were used to generate three reflectance algorithms. Reflectance at 550 nm was used because plants in general have strong reflectance in the green region due to the low absorption of radiant energy by chlorophyll. Reflectance at 685 nm was used because this region is aligned with the maximum absorption of light by chlorophyll in plants. Thus, any loss in chlorophyll levels in the peppers should cause an observable increase in reflectance at this band. In addition, the 760 nm band was used because, beginning at about 750–760 nm, the NIR reflectance of a plant reaches a plateau. In general, plants under stress that lose leaf biomass and/or chlorophyll concentrations in leaves will exhibit increases in reflectance at 550 and 685 nm, and decreases in reflectance in the NIR region near 760 nm (Buschmann & Nagel 1993; Carter 1993, 1994; Gitelson & Merzlyak 1996, 1997; Lichtenthaler *et al.* 1996). The reflectance band algorithms R760/R550, R760/R685, and NDVI were then generated for all pepper plants. The NDVI indices were generated with the following formula:

$$NDVI = (R760 - R685)/(R760 + R685) \quad [2]$$

https://doi.org/10.1017/S1473550406003053 Published online by Cambridge University Press

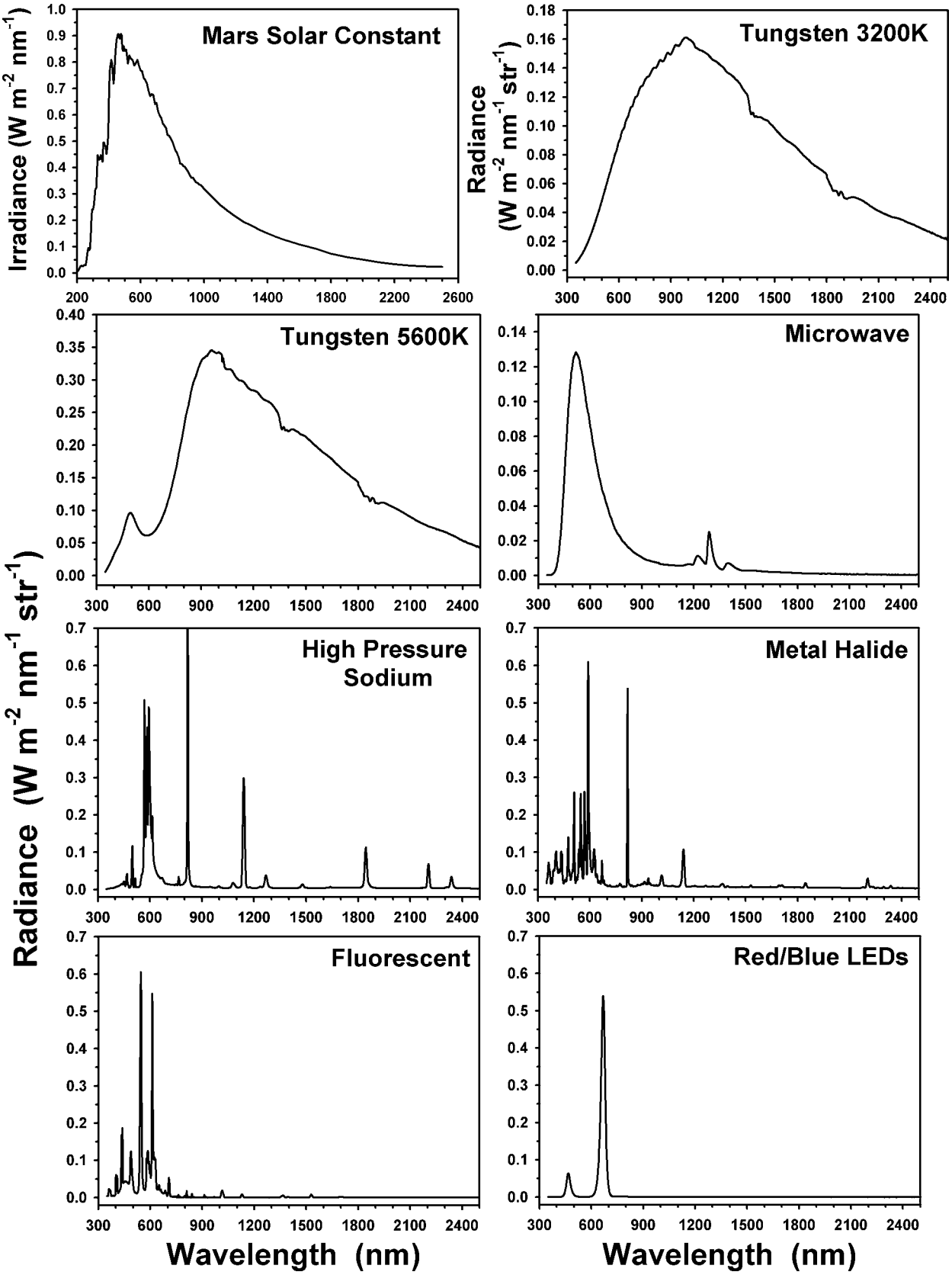

Fig. 2. Spectra for a simulated Mars Solar constant and all seven artificial light sources: The Mars Solar constant was modelled from Schuerger *et al*. (2003), and the spectral scans of the seven artificial light sources were collected as reflectance spectra off of a 99% Spectralon target set at identical photon flux densities of 300 μmol m^{-2} s^{-1} PAR.

https://doi.org/10.1017/S1473550406003053 Published online by Cambridge University Press

Table 1. *Spectral characteristics of FL, MH, HPS, red/blue LEDs, MCW, tungsten halogen 3200K (T3200), and tungsten halogen 5600K (T5600) lamps measured with an Eppley PSP pyranometer (800–3000 nm) and an Eppley PIR pyrgeometer (3000–50 000 nm)*

Spectral range (nm)	Lamp type Irradiance (W m^{-2})[a]						
	LED	MCW	MH	FL	HPS	T3200	T5600
300–715	56.3	68.8	77.1	81.1	63.1	67.8	77.2
715–3000	0.5	25.1	45.8	6.6	61.4	417.4	799.8
300–3000	56.8	93.9	122.9	87.8	124.5	485.2	877.0
3000–50 000	4.5	11.7	11.7	68.6	92.9	40.2	11.7
300–50 000	61.3	105.6	134.6	156.4	217.4	525.4	888.8

[a] All Eppley pyranometer and pyrgeometer measurements were conducted with the photosynthetically active Radiation (PAR; 400–700 nm) adjusted to approximately 300 μmol m^{-2} s^{-1} (≈63 W m^{-2}) at the tops of the sensors, as measured by a handheld quantum sensor (model LI-250A, Li-COR, Lincoln, NE, USA).

Table 2. *Plant biometric data for pepper* (Capsicum annuum *L.*) *plants grown with 100, 50, 25, or 10% NS*

NS	Plant height (cm)	Total chlorophyll (μg/cm^2)	Number of leaves per plant	Leaf fresh weight (g)	Leaf area (cm^2)
100%	14.2 a[a]	57.0 a	15.9 a	12.3 a	322.5 a
50%	14.8 b	38.8 b	11.4 b	6.1 b	181.9 b
25%	11.7 c	25.1 c	9.0 c	2.2 c	71.7 c
10%	8.5 c	19.7 d	6.2 d	0.7 d	28.3 d

[a] Data were log-transformed prior to ANOVA and protected least-squares mean separation tests ($P \leqslant 0.05$, $n = 10$); table values are untransformed means of data. Treatments in columns with similar letters were not significantly different.

Statistical procedures

Statistical analyses were conducted with the PC-based Statistical Analysis System (SAS Institute, Cary, NC, USA). A completely randomized experimental design was used to grow plants in the M-15 growth chamber. Plant biometric data required a log-transformation prior to analyses, but data in Table 2 are given as untransformed numbers. In contrast, all remote sensing data did not require transformation prior to analyses. Plant biometric data were analysed with ANOVA and protected least-squares mean separation tests ($P \leqslant 0.05$) using PROC GLM in SAS. Remote sensing data were analysed with linear regression models using PROC REG in SAS; probability (P) values and residuals (r^2) for all models are given in the appropriate tables. The experiment was conducted twice with five plants per nutrient level per experiment ($n = 10$).

Results

Pepper plants exhibited a strong response to the reduction of nutrients in the hydroponic solutions used in this study. Control plants exhibited large mature canopies of dark green leaves, while plants grown at 50, 25, or 10% nutrient concentrations exhibited increasing levels of chlorosis and stunting (Fig. 1(d) and Table 2). All plant biometric measurements of the pepper plants collected at the end of both experiments exhibited strong linear decreases in plant height total leaf chlorophyll concentrations, numbers of leaves per plant, leaf fresh weights, and leaf areas (Table 2). The greatest changes were observed between 50 is 10% nutrient levels. By all measurements, the peppers grown at 25 and 10% nutrient levels exhibited strong stress symptoms typical of plants grown under severe nutrient deficiencies.

Prior to conducting the remote sensing measurements of healthy and stressed pepper canopies, three energy measurements of the seven artificial light sources were completed. First, the reflectance spectra from the 3200K, 5600K, MCW, HPS, MH, FL, and LED lamps were measured off of a 99% Spectralon reflectance panel (Fig. 2), and compared to an estimate of the Mars solar constant (modelled from Schuerger *et al.* (2003)). The 3200K, 5600K, and MCW lamps were the closest matches to the Mars solar constant of the seven lamps measured. The HPS, MH, and FL lamps exhibited multiple emission peaks at various wavelengths of light throughout the range of 350 to 2500 nm. However, the FL lamps exhibited most of the light output in the region from 350 to 800 nm. The red/blue LED arrays exhibited only two emission peaks at 460 and 660 nm. Lastly, although it is not obvious in the plots given in Fig. 2, there was very little to zero light output for the MCW, MH, and FL lamps above 1800 nm, and nearly zero light output for the LED lamps above 800 nm.

Second, the energy outputs of the seven lamps were measured by three different instruments to characterize NIR and ThIR outputs of the light sources (Table 1). Data in Table 1 are organized from left to right to represent the lowest to highest energy signatures of the seven lamps. The lowest NIR (715–3000 nm) signature was observed in the red/blue LED arrays (0.5 W m^{-2}), and the highest NIR signature was observed for the 5600K lights (799.8 W m^{-2}). The ThIR signatures (3000–50 000 nm) for LED, MCW, MH, and 5600K lamps were similar and ranged from 4.5 to 11.7 W m^{-2}. However, the HPS, FL, and 3200K lamps exhibited significantly higher ThIR signatures that ranged from 92.9 to 40.2 W m^{-2}, respectively. Thus, the LED arrays had the lowest, and the tungsten 5600K lamps had the highest overall heat signatures of the seven lamps. These results are consistent with a previous study comparing the thermal signatures of MH and LED lamps (Brown *et al.* 1995).

Third, the power output rates of the lamps were measured with a DC-voltage oscilloscope in order to determine if their light output varied in time (Fig. 3). The AC-powered HPS, MCW, MH, and tungsten lamps exhibited power fluctuations at approximately 120 Hz that represented the effects of AC on their light outputs. However, the light fluctuations were significantly greater for the HPS and MH lamps because these lamps generate light as arcs across a bridged filament. The AC-powered MCW and tungsten lamps had significantly

https://doi.org/10.1017/S1473550406003053 Published online by Cambridge University Press

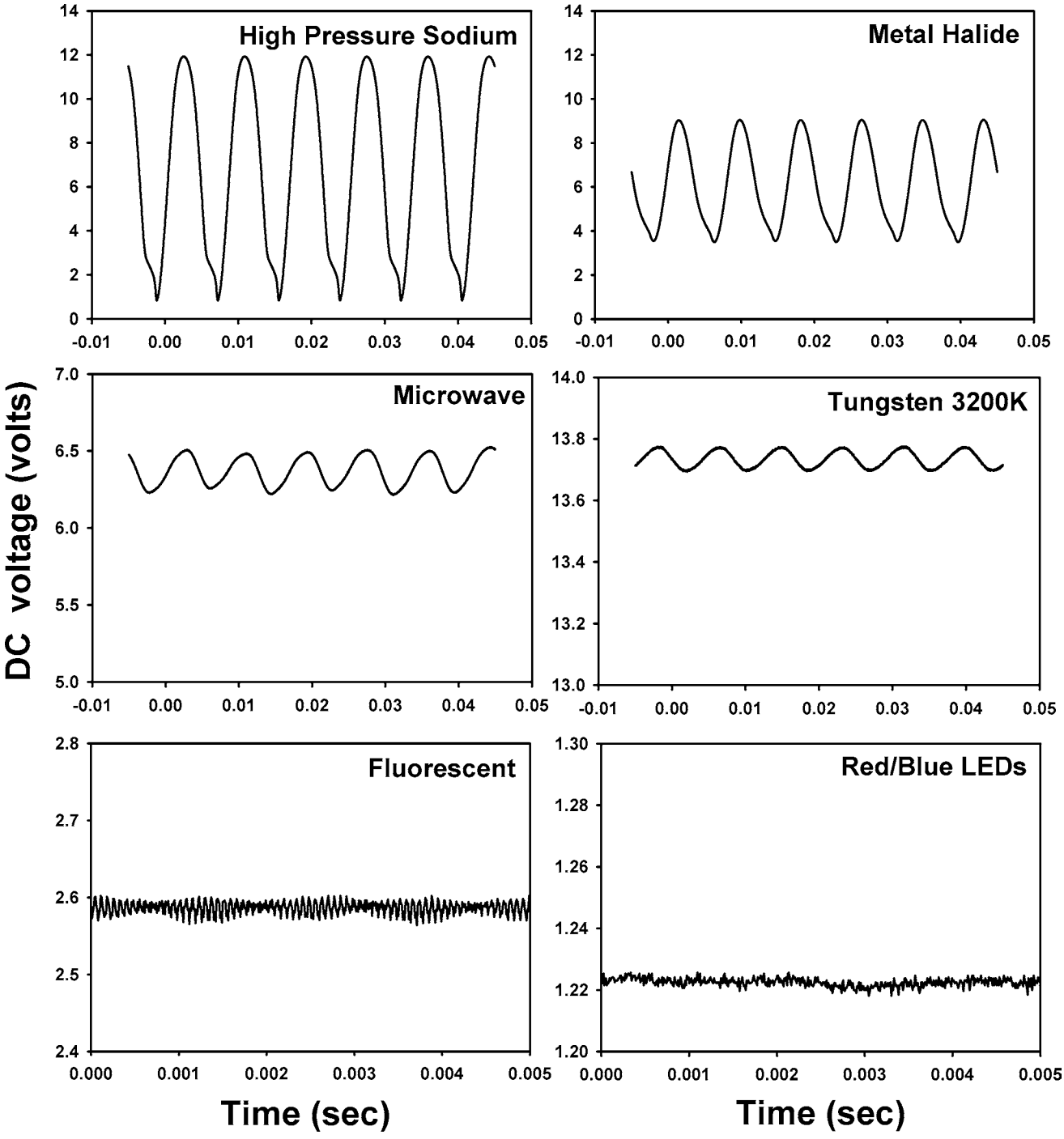

Fig. 3. Voltage output (DC) from a solar panel illuminated with 300 μmol m^{-2} s^{-1} PAR visible light from seven artificial light sources: The AC-powered HPS and MH lamps exhibited the greatest fluctuations in voltage. The AC-powered MCW and 3200K lamps exhibited significantly smaller voltage fluctuations than the HPS and MH lamps. The DC-powered FL and red/blue LED lamps exhibited very small voltage fluctuations.

lower fluctuations in light output as compared to the HPS and MH lamps. In addition, the DC-powered FL and LED lamps exhibited the lowest fluctuations (less than ± 0.05 V from peak to trough) in light output. The tungsten, MCW, FL, and LED lamps were the most stable illumination sources tested. In contrast, the HPS and MH arc lamps produced strongly fluctuating light outputs. Because the HPS and MH exhibited such strongly fluctuating light outputs, short integration times and low scan averages, when using the ASD Field-Spec Pro spectroradiometer to measure plant, yielded wildly changing spectra. Thus, the ASD spectroradiometer was operated with long integration times per scan and 25

https://doi.org/10.1017/S1473550406003053 Published online by Cambridge University Press

spectral scans were averaged per saved spectrum in order to reduce the extreme fluctuations in light output by the HPS and MH lamps.

Spectral scans from a single healthy pepper canopy were measured to compare the reflectance spectra collected under the seven artificial lamps (Fig. 4). The orientation of the pepper canopy to the lamps was held constant, and the measurements in Fig. 4 were collected within 60 mins of each other on a single day. Thus, the differences among the various reflectance spectra represent differences due to the illumination sources, and not due to plant canopy, time, or spectroradiometer changes. The spectra of the tungsten 3200K and 5600K lamps were the smoothest of all illumination sources, and are typical of what is expected from healthy plant canopies (Buschmann & Nagel 1993; Carter 1993, 1994; Gitelson & Merzlyak, 1996, 1997; Lichtenthaler *et al*. 1996).

The MCW lamp exhibited a smooth reflectance spectrum from 400 to 1700 nm, and was very similar to the reflectance spectra collected with the 3200K and 5600K lamps, although the reflectance values were slightly lower. However, the MCW lamp had significant levels of noise in the spectrum from 350 to 400 nm and from 1700 to 2500 nm. Comparing this result with the amount of photon flux from the lamps measured as the reflectance off of a 99% reflectance target (Fig. 2), the most likely causes of the noise in these channels were low amounts of photon flux outputs in these regions.

Similar to the MCW lamp, the reflectance spectra from the HPS, MH, and FL lamps exhibited increased noise in the 1700 to 2500 nm region that was due primarily to low photon flux outputs of the lamps in this region. In addition, the reflectance spectra from HPS, MH, and FL lamps in the 350 to 1200 nm region exhibited a marked increase in fluctuations due to the influence of the individual emission peaks of these lamps in this region (see Fig. 2). Thus, the reflectance spectra from the HPS, MH, and FL lamps were significantly degraded compared to the 3200K, 5600K, and MCW lamps.

In contrast to all other lamps, the reflectance spectra from the red/blue LED arrays were very different in spectral quality along the entire range of 350 to 2500 nm (Fig. 4). First, from 800 to 2500 nm, the reflectance spectrum is composed of non-interpretable noise caused by a complete lack of photon flux output in the LED arrays in this region. Second, the spectral region from 400 to 800 nm exhibited two peaks centred at 550 and 740 nm that likely represent the fluorescence of carotene and xanthophyll at 550 nm and chlorophyll at 740 nm (Lichtenthaler 1996; Richards *et al*. 2003). The green fluorescence at 550 nm was likely induced by the blue LEDs centred at 460 nm, and the NIR fluorescence at 740 nm was likely induced by both the blue and red LEDs in the lamp array.

The next step in evaluating the effectiveness of these seven artificial lamps for remote sensing measurements in bioregenerative ALS systems was to determine whether the reflectance spectra from the seven lamps could be used to detect plant stress and estimate both chlorophyll concentration and leaf area of healthy and nutritionally stressed peppers. The reflectance spectra from the seven artificial lamps were grouped into three distinct clusters. First, the most stable and easily interpretable spectra were grouped together (Fig. 5). Reflectance spectra from the 3200K, 5600K, and MCW lamps followed closely similar trends in which the reflectance at 550 and 685 nm increased, and the reflectance at 760 nm decreased, in plants grown under increasingly severe nutritional stress. In general, the increases in reflectance at 550 and 685 nm, and the decreases in reflectance at 760 nm, followed linear models (Table 3) in which the P values were highly significant, and the residuals (r^2) were generally high. The table values for these bands were very similar among the 3200K, 5600K, and MCW lamps (Table 3).

Second, reflectance spectra that were somewhat degraded, compared to the traditionally clean reflectance spectra from a 3200K lamp, were grouped together (Fig. 6). In this cluster, the subtle changes in reflectance at 550, 685, and 760 nm by the HPS, MH, and FL lamps were somewhat difficult to interpret, but when quantitatively analysed (Table 3) exhibited similar trends as the first cluster of lamps (Fig. 5). The easiest to interpret were the MH reflectance spectra of the pepper plants in which the reflectance at 550 and 685 nm increased, and the reflectance at 760 nm generally decreased in plants grown under increasingly more severe nutritional stress. However, the HPS, and in particular the FL, reflectance spectra were very difficult to interpret due to a compression of the spectra onto one another. Furthermore, the reflectance spectra of all three lamps in this cluster (MH, HPS, and FL) were degraded by the influence of the emission peaks in the illumination sources (see Fig. 2). Thus, the general trends of increasing reflectance in the 550 and 685 nm regions, and the decreasing reflectance in the 760 nm region, were similar to the spectra collected with the 3200K lamp, but fluctuations due to interference from emission peaks of the lamps, and the lack of photon flux outputs in some regions, significantly degraded the reflectance spectra from the MH, HPS, and FL lamps.

Third, the spectra from the red/blue LED lamps of healthy and nutritionally stressed pepper plants diverged dramatically from the reflectance spectra from the other artificial light sources and were plotted separately (Fig. 7). At first inspection, the spectra of the LED lamps are practically uninterpretable (Fig. 7(a)). As discussed above for a single healthy plant canopy, the regions from 350 to 400 nm and from 800 to 2500 nm are composed entirely of random fluctuations caused by errors in the algorithms used by the ASD FieldSpec Pro spectroradiometer to estimate spectral reflectance. These errors are due to the complete lack of photon flux output in these regions by the red and blue LEDs. Thus, the only plausible useful region is from 400 to 800 nm. However, even here (Fig. 7(b)), the results are counterintuitive. The spectra for the LEDs do not match typical reflectance spectra of plants illuminated with natural or artificial lights, and we interpret the peaks at 550 and 740 nm to be fluorescence peaks associated with emissions from carotene, xanthophyll,

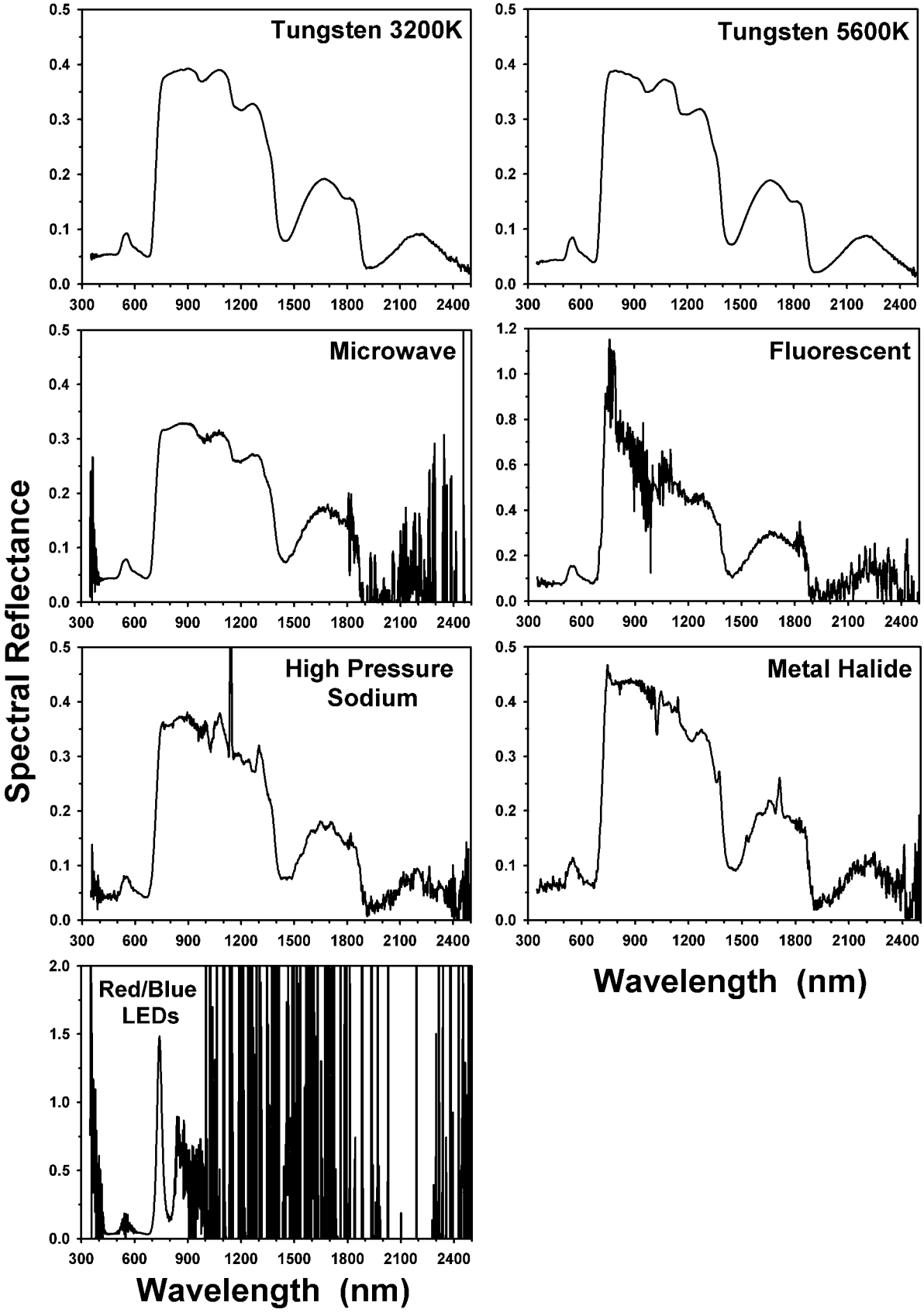

Fig. 4. Spectroradiometer scans under seven artificial lamps of a single control pepper plant grown at a 100% nutrient level: The alignment of the plant canopy was identical for all measurements. The spectra were collected with the ASD Field-Spec Pro and were averages of 25 spectral scans.

https://doi.org/10.1017/S1473550406003053 Published online by Cambridge University Press

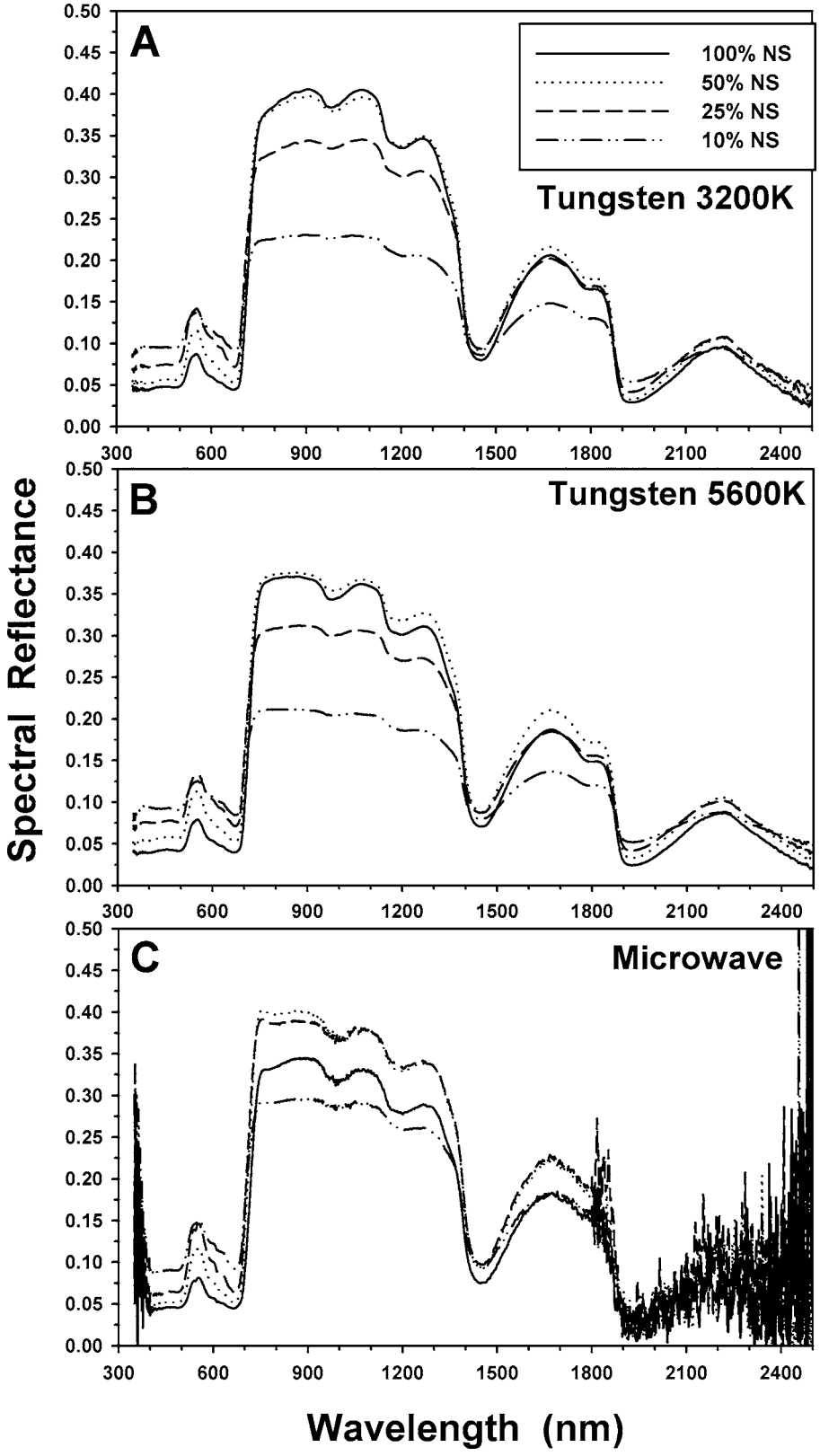

Fig. 5. Reflectance spectra for all pepper (*Capsicum annuum* L.) plants ($n = 10$) collected under the 3200K, 5600K, and MCW lamps. (A) Reflectance spectra of plant canopies under the 3200K lamps were considered as the industry standard controls. (B) Reflectance spectra of pepper plants under 5600K illumination wave generated using a dichroic filter placed in the light path of the 3200K lamps. (C) Reflectance spectra of pepper plants under the MCW lamp are similar to both the 3200K and 5600K spectra except that there is greater noise in the spectral region from 1800 to 2500 nm due to low light fluence rates in the MCW lamp.

https://doi.org/10.1017/S1473550406003053 Published online by Cambridge University Press

Table 3. *Effects of illumination source on the spectral reflectance of pepper plants* (Capsicum annuum *L.*) *under nutritional stress*

Lamp	Reflectance band (nm)	100%NS	50% NS	25% NS	10%NS	Linear models[a]	*P* values	r^2 values
Tungsten 3200K	550	0.0869	0.1154	0.1412	0.1370	$y=-0.0006x+0.149$	<0.0001	0.6436
	685	0.0486	0.0578	0.0793	0.0970	$y=-0.0005x+0.094$	<0.0001	0.6320
	760	0.3718	0.3715	0.3232	0.2241	$y=0.0013x+0.263$	<0.0001	0.4005
	R760/R550	4.32	3.23	2.27	1.64	$y=0.0291x-1.53$	<0.0001	0.9121
	R760/R685	7.80	6.55	4.05	2.36	$y=0.0577x+2.54$	<0.0001	0.7709
	NDVI	0.7695	0.7298	0.6014	0.3976	$y=0.0035x+0.464$	<0.0001	0.6607
Tungsten 5600K	550	0.0788	0.1130	0.1335	0.1251	$y=-0.0006x+0.140$	0.0001	0.5662
	685	0.0436	0.0580	0.0786	0.0899	$y=-0.0005x+0.091$	<0.0001	0.6616
	760	0.3609	0.3683	0.3050	0.2106	$y=0.0014x+0.248$	<0.0001	0.4033
	R760/R550	4.59	3.26	2.28	1.69	$y=0.0319x+1.48$	<0.0001	0.9523
	R760/R685	8.33	6.43	3.88	2.36	$y=0.0646x+2.27$	<0.0001	0.8528
	NDVI	0.7828	0.7261	0.5888	0.4028	$y=0.0037x+0.455$	<0.0001	0.7398
MCW	550	0.0807	0.1157	0.1447	0.1498	$y=-0.0008x+0.159$	<0.0001	0.8836
	685	0.0512	0.0622	0.0754	0.1015	$y=-0.0005x+0.095$	<0.0001	0.7370
	760	0.3306	0.4030	0.3907	0.2920	$y=0.00008x+0.350$	NS	0.0027
	R760/R550	4.12	3.47	2.70	1.95	$y=0.0228x+2.01$	<0.0001	0.8452
	R760/R685	6.51	6.52	5.19	2.88	$y=0.0342x+3.69$	0.0004	0.5151
	NDVI	0.7315	0.7288	0.6755	0.4837	$y=0.0022x+0.554$	0.0005	0.5020
HPS	550	0.0735	0.0875	0.1153	0.1022	$y=-0.0004x+0.114$	<0.0001	0.3580
	685	0.0618	0.0635	0.0799	0.0815	$y=-0.0002x+0.082$	0.0046	0.1977
	760	0.3285	0.3364	0.3004	0.1864	$y=0.0012x+0.234$	0.0012	0.2490
	R760/R550	4.54	3.83	2.58	1.82	$y=0.0292x+1.85$	<0.0001	0.8411
	R760/R685	5.62	5.26	3.73	2.30	$y=0.0335x+2.70$	<0.0001	0.6498
	NDVI	0.6899	0.6787	0.5746	0.3918	$y=0.0028x+0.459$	<0.0001	0.5779
MH	550	0.0751	0.1033	0.1240	0.1229	$y=-0.0006x+0.133$	<0.0001	0.4201
	685	0.0559	0.0692	0.0915	0.1082	$y=-0.0006x+0.107$	0.0046	0.4384
	760	0.3499	0.3736	0.3464	0.2426	$y=0.0008x+0.291$	NS	0.0865
	R760/R550	4.69	3.61	2.75	1.96	$y=0.0289x+1.92$	<0.0001	0.8880
	R760/R685	6.44	5.45	3.73	2.27	$y=0.0434x+2.48$	<0.0001	0.7671
	NDVI	0.7281	0.6859	0.5739	0.3866	$y=0.0033x+0.446$	<0.0001	0.6787
FL	550	0.1524	0.1455	0.1651	0.1010	$y=0.0003x+0.127$	NS	0.0902
	685	0.1142	0.1051	0.1276	0.0878	$y=0.0001x+0.103$	NS	0.0311
	760	0.9741	0.8766	0.6920	0.2989	$y=0.0063x+0.424$	<0.0001	0.4394
	R760/R550	6.43	6.02	4.18	2.95	$y=0.0289x+1.92$	<0.0001	0.5218
	R760/R685	8.48	8.25	5.43	3.37	$y=0.0525x+3.98$	<0.0001	0.5450
	NDVI	0.7878	0.7753	0.6716	0.5348	$y=0.0024x+0.582$	<0.0001	0.5291
Red/blue LEDs	550	0.0784	0.0795	0.1322	0.1351	$y=-0.0007x+0.138$	<0.0001	0.3648
	685	0.0370	0.0453	0.0511	0.0685	$y=-0.0003x+0.064$	<0.0001	0.5064
	760	0.8941	1.0303	0.7479	0.5413	$y=0.0034x+0.649$	0.0016	0.2391
	R760/R550	15.9	14.08	5.73	4.11	$y=0.1358x+3.71$	0.0008	0.2652
	R760/R685	25.06	23.52	15.06	8.45	$y=0.1706x+10.22$	<0.0001	0.4588
	NDVI	0.9161	0.915	0.8689	0.7520	$y=0.0014x+0.798$	<0.0001	0.3771

[a] Data were not transformed prior to analyses. Linear regression models were generated by PROC REG in SAS; *P* values represent the levels of significance for the overall model ($n=10$).

and chlorophyll (Lichtenthaler 1996; Richards *et al*. 2003). We believe that the 550 and 740 nm peaks from the LED lamps are fluorescence peaks of pepper leaves for the following three reasons: (a) the peaks at 550 and 740 nm match fluorescence peaks previously published for dicotyledonous plants such as pepper (Lichtenthaler 1996; Richards *et al*. 2003), (b) the 740 nm peak does not match any reflectance spectra reviewed in the literature with plants illuminated with natural or artificial light sources (see Buschmann & Nagel (1993); Carter (1993), (1994); Gitelson & Merzlyak (1996), (1997), Lichtenthaler *et al*. (1996) and the citations within these reports), and (c) the red/blue LED arrays did not produce any significant photons at 550 and 740 nm, and, thus, we would not expect to see any reflected photons in the corresponding reflectance spectrum. However, one caveat to this interpretation is appropriate. In general, chlorophyll fluorescence is composed of two fluorescence peaks centred at 680 and 740 nm (Lichtenthaler 1996). However, the spectrum given in Fig. 7 for the red/blue LED array lacks the first peak at 680 nm. We do not have an explanation for this, but suggest that the problem might arise from the use of red LEDs centred at 660 nm as an illumination source. It is

https://doi.org/10.1017/S1473550406003053 Published online by Cambridge University Press

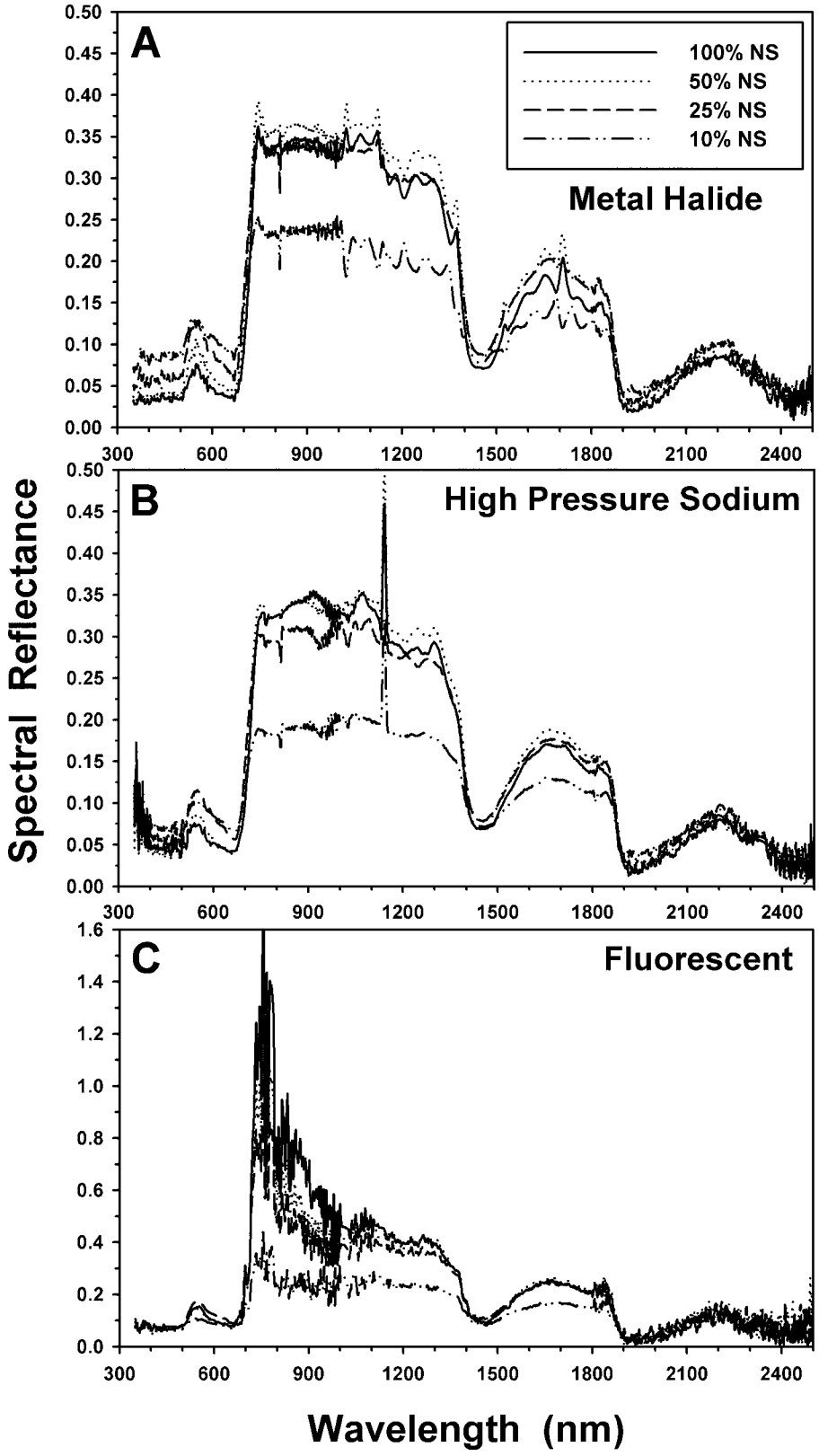

Fig. 6. Reflectance spectra for all pepper (*Capsicum annuum* L.) plants ($n = 10$) collected: (A) MH; (B) HPS; (C) FL. The reflectance spectra of these three lamps were strongly influenced by the emission peaks present in the original light sources (see Fig. 3), and resulted in reduced clarity of the spectral differences among peppers grown at the different levels of nutrients.

https://doi.org/10.1017/S1473550406003053 Published online by Cambridge University Press

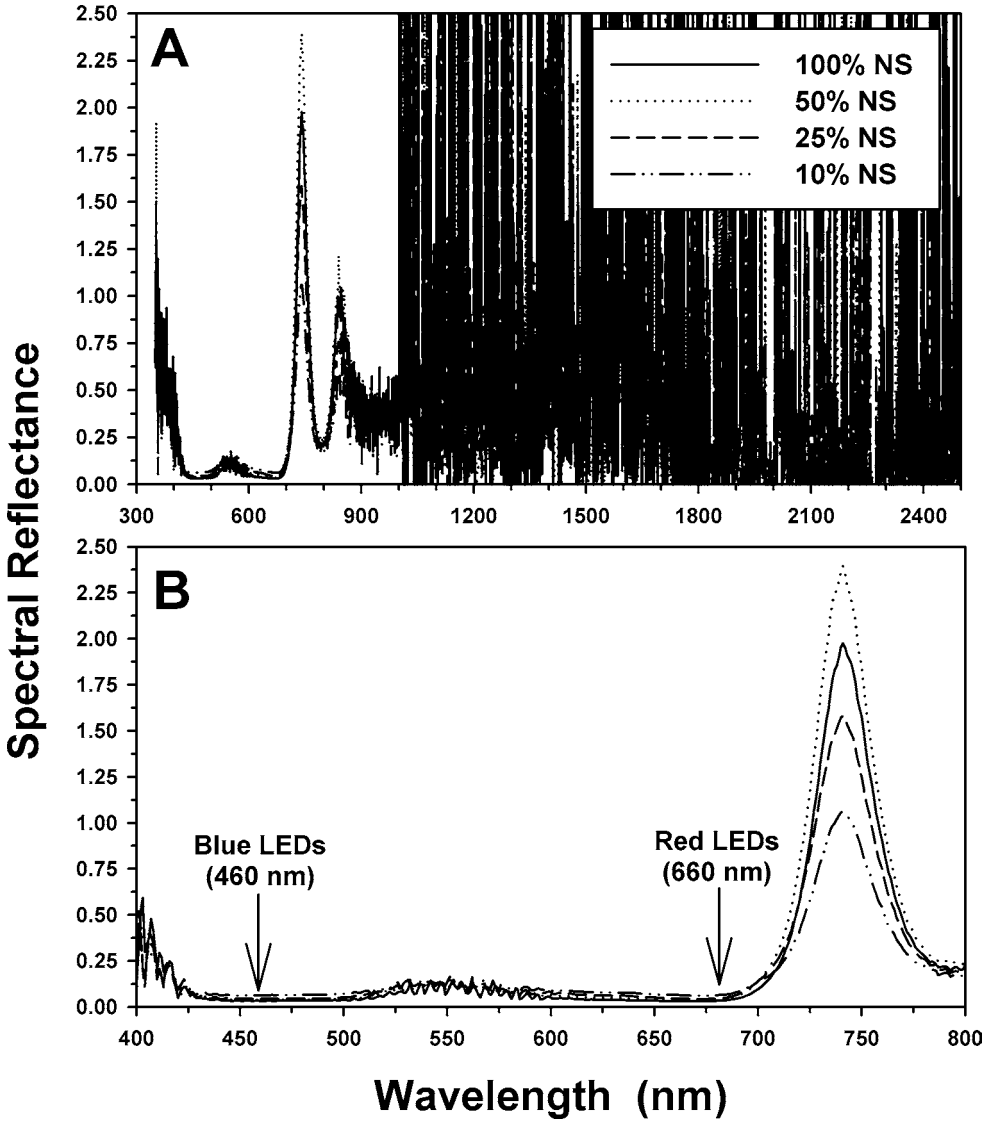

Fig. 7. Spectra of pepper (*Capsicum annuum* L.) plants ($n = 10$) collected under the red/blue LEDs. (A) Full-range (350–2500 nm) reflectance spectra of peppers grown at 100, 50, 25, or 10% nutrient levels exhibiting a severe loss of the reflectance signal of plants from 800 to 2500 nm due to the absence of photons in this region from the LED arrays. (B) Data from (a) re-graphed at a constrained spectral range of 400–800 nm. Blue (460 nm) and red (660 nm) illumination is not observed here because these regions are where maximum absorption of light energy is achieved by chlorophyll. The subtle peaks at 550 nm (green region) and at 740 nm (NIR region) represent fluorescence light emitted from carotene and xanthophyll (550 nm peak) and from chlorophyll (740 nm peak).

possible that the 660 nm excitation photons are interfering with the 680 nm chlorophyll fluorescence emission photons. We have not analysed these data for the NIR/red chlorophyll fluorescence ratio because there is not yet a clear explanation on why the 680 nm fluorescence band typical of chlorophyll (Lichtenthaler 1996) is absent. Additional tests are required to fully characterize the relationship of excitation and emission photons when LED lighting arrays are used for illuminating plant canopies in ALS systems.

The reflectance values for all seven lamps were used to generate three simple reflectance algorithms; namely R760/R550, R760/R685, and NDVI values. These algorithms were tested with linear regression models against the nutritional levels applied to pepper plants (Fig. 8 and Table 3). The linear models for all seven lamps were all highly significant ($P < 0.01$). However, the residuals for these models differed greatly indicating that some light sources yielded high-quality models for predicting plant stress. First, the linear models for reflectance versus plant stress measured with the LED lamps were consistently divergent from all other lamps tested (Fig. 8). For the three reflectance algorithms, R760/R550, R760/R685, and NDVI, the linear models from the LED lamps were significantly higher than the models from all other lamps exhibiting different slope values and *y*-intercepts (Fig. 8 and Table 3). Second, the most similar and overlapping models tested were those reflectance models for the R760/R550 band ratio when measured under the 3200K, 5600K, MCW, HPS, and MH lamps (Fig. 8(a)). Third, there was close agreement with all lamps, except the LED lamps, for the band ratio R760/R685 (Fig. 8(b)), but there was a wide

https://doi.org/10.1017/S1473550406003053 Published online by Cambridge University Press

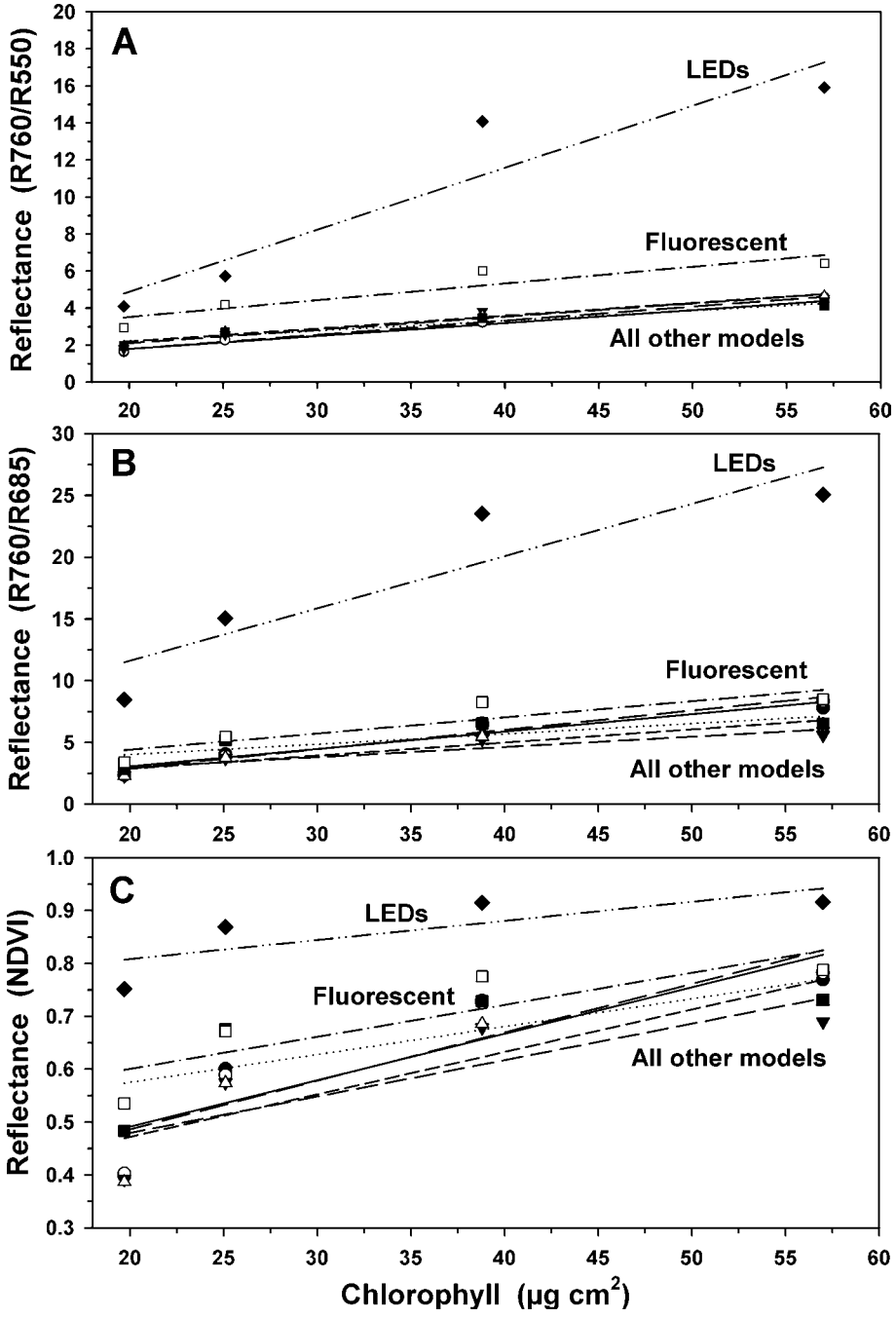

Fig. 8. Linear regression models for correlations between chlorophyll concentrations in pepper (*Capsicum annuum* L.) leaves versus the reflectance algorithms (A) R760/R550, (B) R760/R685, and (C) NDVI (defined as $NDVI = (R760 - R685)/(R760 + R685)$. Models for LEDs were always distinctly different compared to all other models for the three algorithms. The tightest grouping of linear models were for the reflectance algorithm R760/R550 (A) from peppers illuminated with the 3200K, 5600K, MH, HPS, and MCW lamps. The worst overlap of linear models was observed for the NDVI algorithm (C) indicating a lower level of agreement among the seven lamps in which NDVI was used to estimate chlorophyll concentration.

divergence of linear models for NDVI reflectance versus plant stress (Fig. 8(c)). Fourth, the R760/R550 band ratio yielded consistently higher residuals than either the R760/R685 or NDVI algorithms (Table 3). Furthermore, the R760/R550 band ratio exhibited high residuals for all lamps except the FL and LED lamps. Fifth, the highest residuals were observed in the linear models derived from reflectance spectra from the 3200K, 5600K, and MCW lamps, and the lowest residuals were observed for plants measured under FL and LED lamps (Table 3). Finally, although the residuals were significantly lower in both the FL and LED lamps, the linear models were still significant and thus could still be used to predict the levels

https://doi.org/10.1017/S1473550406003053 Published online by Cambridge University Press

Table 4. *Linear regression models comparing chlorophyll concentration of leaves or leaf area to three common reflectance algorithms with pepper plants* (Capsicum annuum *L.*) *grown under nutritional stress*

	Chlorophyll versus reflectance				Leaf area versus reflectance		
Lamp	Reflectance band (nm)	Linear models[a]	*P* values	r^2 values	Linear models	*P* values	r^2 values
Tungsten 3200K	R760/R550	$y=0.0663x+0.541$	<0.0001	0.8893	$y=0.0085x+1.58$	<0.0001	0.9451
	R760/R685	$y=0.132x+0.583$	<0.0001	0.7537	$y=0.0176x+2.54$	<0.0001	0.8703
	NDVI	$y=0.008x+0.346$	<0.0001	0.6340	$y=0.0011x+0.469$	<0.0001	0.6989
Tungsten 5600K	R760/R550	$y=0.072x+0.428$	<0.0001	0.9125	$y=0.0092x+1.56$	<0.0001	0.9588
	R760/R685	$y=0.1446x+0.187$	<0.0001	0.8005	$y=0.0194x+2.33$	<0.0001	0.9297
	NDVI	$y=0.0084x+0.333$	<0.0001	0.7043	$y=0.0011x+0.462$	<0.0001	0.7751
MCW	R760/R550	$y=0.0520x+1.19$	<0.0001	0.8237	$y=0.0071x+2.11$	<0.0001	0.7652
	R760/R685	$y=0.0743x+2.60$	0.0011	0.4574	$y=0.0107x+3.84$	0.0008	0.4751
	NDVI	$y=0.0048x+0.483$	0.0011	0.4559	$y=0.00068x+0.563$	0.0010	0.4603
HPS	R760/R550	$y=0.0680x+0.816$	<0.0001	0.8510	$y=0.0085x+1.92$	<0.0001	0.8501
	R760/R685	$y=0.0778x+1.51$	<0.0001	0.6560	$y=0.0097x+2.79$	<0.0001	0.6528
	NDVI	$y=0.0064x+0.363$	<0.0001	0.5764	$y=0.00079x+0.467$	<0.0001	0.5710
MH	R760/R550	$y=0.0677x+0.883$	<0.0001	0.9070	$y=0.0081x+2.03$	<0.0001	0.8419
	R760/R685	$y=0.0999x+0.984$	<0.0001	0.7606	$y=0.0130x+2.53$	<0.0001	0.8298
	NDVI	$y=0.00743x+0.335$	<0.0001	0.6658	$y=0.00095x+0.452$	<0.0001	0.7039
FL	R760/R550	$y=0.0890x+1.79$	<0.0001	0.5805	$y=0.0103x+3.36$	<0.0001	0.5019
	R760/R685	$y=0.1251x+2.02$	<0.0001	0.5789	$y=0.0146x+4.21$	<0.0001	0.5075
	NDVI	$y=0.00583x+0.489$	<0.0001	0.5704	$y=0.00068x+0.591$	<0.0001	0.5047
Red/blue LEDs	R760/R550	$y=0.319x-1.21$	0.0006	0.2737	$y=0.0418x+3.67$	0.0003	0.3029
	R760/R685	$y=0.371x+5.07$	<0.0001	0.4082	$y=0.0563x+9.58$	<0.0001	0.6038
	NDVI	$y=0.0032x+0.751$	<0.0001	0.3562	$y=0.00043x+0.799$	<0.0001	0.4141

[a] Data were not transformed prior to analyses. Linear regression models were generated by PROC REG in SAS; *P* values represent the levels of significance for the overall model ($n=10$).

of nutritional stress in pepper plants, albeit with lower confidence than the other light sources.

As plant stress was most dramatically revealed by increases in chlorosis and stunting when peppers were irrigated with low nutrient levels (Fig. 1(d) and Table 2), linear models were tested for the correlation between changes in the reflectance algorithms R760/R550, R760/R685, and NDVI and changes in chlorophyll content of leaves and leaf area of plants. These results (Table 4) show similar trends for the utility of these remote sensing algorithms in estimating losses in chlorophyll and leaf biomass caused by severely stressed plant canopies as were observed for the overall effects of nutritional level on pepper growth. In particular, the highest residuals were observed for R760/R550 band ratios estimated from data collected under the 3200K, 5600K, MCW, HPS, and MH lamps. The lowest residuals, and thus the lowest predictive capabilities, were observed for the FL and LED lamps. However, all models were significant ($P<0.01$) and thus all lamps could be used to estimate losses in chlorophyll and leaf biomass caused by nutritional stresses in bioregenerative ALS systems, albeit with lower confidence for the FL and LED lamps.

Discussion

The reduction of the ESM in bioregenerative ALS systems is a critical component of enhancing the utility of such systems for future human missions to the Moon and Mars. One way of reducing the ESM in an ALS module would be to deploy an automatic crop monitoring system that would notify the crew and ground technicians only when the plants deviate from an accepted 'nominal range' of productivity. Towards this end, the current study sought to determine the effectiveness of seven artificial illumination sources for remote sensing measurements of healthy and nutritionally stressed plant canopies. A key goal was to determine if any one type of illumination had any over-arching negative qualities that would preclude its use as a light source in bioregenerative ALS systems. All seven illumination systems were chosen based on previous reports on their utility in ALS crop production (see Olson *et al.* (1988); Bula *et al.* (1991); Barta *et al.* (1992); Brown *et al.* (1995); Goins *et al.* (1997); Schuerger & Brown (1997); Goins & Yorio (2000); Wheeler & Martin-Brennan (2000); Wheeler *et al.* (2003); Kim *et al.* (2004a), (b) and the citations within these reports).

Tungsten halogen lamps (both 3200K and 5600K sources) exhibited consistently higher residuals for linear models with the R760/R550, R760/R685, and NDVI algorithms. These illumination sources yielded smooth and easily interpretable spectra of healthy and stressed plant canopies across the full range of the reflectance spectra measured here (from 350 to 2500 nm). The linear models from these two lamps were highly correlated to changes in nutrient level, chlorophyll, and leaf area. In contrast, the AC-powered MCW, HPS, and MH, and the DC-powered FL lamp typically had regions of the reflectance spectrum that were not useable and exhibited generally lower residuals for linear models of the three

https://doi.org/10.1017/S1473550406003053 Published online by Cambridge University Press

algorithms than the tungsten halogen lamps. Of all seven artificial lamps tested, the red/blue LED arrays yielded significant ($P \leqslant 0.05$) linear models for correlations to nutritional stress, chlorophyll concentration, and leaf area; but had generally much lower residuals than all other lamps.

Based on the above summary alone, one might conclude that tungsten halogen lamps are the preferred choice for collecting remote sensing signatures of plants in ALS canopies. However, both the 3200K and 5600K tungsten halogen lamps had one single flaw that renders them questionable as a remote sensing light source in ALS modules. The heat signatures of the tungsten halogen lamps were dramatically higher than all other light sources tested (Table 1), and, thus, would be expected to add significant thermal loads on plant canopies during remote sensing measurements. In fact, the total thermal signature for the 5600K tungsten halogen lamp was over an order-of-magnitude greater than the thermal signatures of the red/blue LED arrays. The added thermal loading might be sufficient to increase the ESM of the ALS system by requiring additional cooling capacity, and, thus, drive the economic justification down for using bioregenerative ALS plant production technologies in human missions to Mars. There are perhaps two ways to solve the potential thermal issues with tungsten halogen lamps. First, the frequency in illuminating plant canopies might be reduced in number and duration. Second, the intensity of the tungsten halogen lamps could be reduced in order to lower the thermal heating of plant canopies. However, both approaches would reduce the utility of an automatic plant monitoring system in a bioregenerative ALS by constraining the duration and frequencies of monitoring plants.

The AC-powered MCW, HPS, and MH lamps, and the DC-powered FL lamps, all had reduced thermal signatures compared to the 3200K and 5600K tungsten lamps, but there were several disadvantages of these lamps. First, all four lamps exhibited increased noise in the regions from 350–400 nm and from 1800–2500 nm. These artifacts are likely due to the presence of very low numbers of photons in the light sources at these bands resulting in anomalous readings with the ASD Field Spec Pro spectroradiometer (see the ASD Field Spec Pro user manual). In addition, the many spectral emission bands in the HPS, MH, and FL lamps (Fig. 2) contributed to an increased noise in the important NIR band from 750–1300 nm (Fig. 4). The increased amounts of noise in the NIR band for the HPS, MH, and FL lamps contributed to the reductions in the model residuals for the algorithms R760/R550, R760/R685, and NDVI tested against nutrient levels, chlorophyll concentration, and leaf area. Furthermore, for the HPS and MH lamps, the light outputs were influenced by the fact that both illumination sources utilized electrical arcs across filament bridges to produce photons, and these arcing processes induced dramatic changes in the light outputs of these lamps (Fig. 3). The 120 Hz cycling of the light outputs from the HPS and MH lamps requires that the integration time and number of averaged spectra per saved spectrum are lengthened; thus increasing the time required for collecting spectral data under these lamps. Although this might not be a problem in small plant production systems, it may preclude the use of these lamps if plant monitoring has to be either very frequent or has to cover a large number of measurement sites.

The red/blue LED arrays were unique among the various artificial lighting systems tested in these experiments for three reasons. First, the red/blue LED arrays had the lowest heat signature of all lamps tested, and thus would be expected to lower the ESM of an ALS system significantly if LED technologies would be used either as the primary light source for plant production or as a separate lighting system tailored for remote sensing measurements. This advantage has been used to promote the use of LED technologies for bioregenerative ALS plant production (Bula *et al.* 1991; Barta *et al.* 1992; Brown *et al.* 1995; Goins *et al.* 1997; Schuerger & Brown 1997; Goins & Yorio 2000; Wheeler & Martin-Brennan 2000; Wheeler *et al.* 2003; Kim *et al.* 2004a). Second, the red/blue LED arrays used here yielded the lowest residuals of any lamps tested for the linear models that compared the algorithms R760/R550, R760/R685, and NDVI against the plant biometric measurements of nutrient levels, chlorophyll concentration, and leaf area. Thus, this configuration of red/blue LEDs did not function adequately for detecting plant stress in the nutritionally stressed peppers. Third, most of the spectrum from the LED measured plants was completely unusable (Fig. 7). All wavelengths above 800 nm were unusable due to the complete lack of photons in the source illumination. In addition, the spectrum from 450 to 800 nm (Fig. 7(b)) was very atypical and did not match normal reflectance spectra of dicotyledonous plants such as pepper (Lillesand & Kieffer 1994; Lichtenthaler 1996; Schowengerdt 1997; Richards *et al.* 2003). However, the spectrum for the red/blue LED arrays does match a portion of a typical spectrum of leaf fluorescence obtained from dicotyledonous plants similar to pepper (see Lichtenthaler 1996; Richards *et al.* 2003). In a typical leaf fluorescence spectrum of a dicotyledonous plant, chlorophyll will show two strong fluorescent bands at 685 and 740 nm if excited by light at any wavelength shorter than about 640 nm. We currently believe that the spectrum for the LED arrays reported here represents the NIR fluorescent band at 740 nm, and that the fluorescent band at 685 nm is absent because the excitation light from the red LEDs (at 660 nm) masked the fluorescence emission band at 685 nm. In addition, the green band centred at 550 nm (Fig. 7(b)) matches the green fluorescent band created by the plant pigments, carotene and xanthophyll, excited by blue light (Lichtenthaler 1996; Richards *et al.* 2003).

Based on the quality of the reflectance spectra alone, the tungsten lamps appeared to produce the most easily interpretable reflectance spectra of plants under stress, but the aforementioned thermal heat signatures of the tungsten lamps may preclude their use in ALS systems. In contrast, the heat signatures were lower for the MCW, HPS, MH, and FL lamps, and these lamps can be used directly to grow the plants in ALS modules. However, the reflectance spectra of plants measured under the MCW, HPS, MH, or FL lamps exhibited

reduced stabilities and may not be as accurate in detecting plant stress as the tungsten lamps. Furthermore, at first glance, the LED arrays appeared to be nearly unusable for measuring the reflectance spectra of stressed plants. What then might be an optimum approach for monitoring plant health in a future ALS system on the Moon or Mars through remote sensing?

First, if ALS plant-growth modules utilize natural solar irradiation, then the solar spectrum would be the ideal light source to use for a remote sensing plant monitoring system. However, the thermal issues and light capture issues of such an ALS module might increase the ESM of the system to such a point as to preclude this approach (Olson *et al.* 1988; Wheeler & Martin-Brennan 2000). For example, how the ALS system can actually utilize the natural solar irradiation on Mars is a major question that directly impacts the ESM of a life support system. Olson *et al.* (1988) described several light capturing methods for a Mars ALS system including transparent materials similar to a traditional greenhouse approach, fibre-optic light capturing devices, and light tubes. However, all of these approaches have difficulties. The transparent materials must be very thin, and would require low-pressure environments within the plant growth modules to work (Boston 1981). Furthermore, the fibre-optic and light tubes may significantly raise the ESM of the Mars ALS system based solely on their increased launch mass. Finally, natural insolation on the Moon is only available for 14 days out of every 28 day lunar orbit, and on Mars, the solar constant is only 43% of that found on Earth (Kuhn & Atreya 1979).

Second, the thermal heat signatures of tungsten halogen lamps may preclude them from use as a primary light source for plant productivity. In our experiments, the tungsten halogen lamps often induced plant wilt if the plants were illuminated longer than a few minutes during the remote sensing measurements, and this effect was more pronounced for severely stressed plants grown at 25 or 10% nutrient levels. In addition, the room within which the tungsten halogen lamps were used (Fig. 1) would heat up significantly during the use of the 450 W tungsten halogen lamps. Thus, the times that plants are imaged with a remote sensing system that utilizes tungsten halogen lamps is limited. Recall that these experiments were conducted as part of a program of developing an automatic plant monitoring system that would operate continuously within an ALS plant growth module. The direct experience in the lab during these experiments suggests that high intensity tungsten halogen lamps would add a significant thermal load to an ALS system, and that direct plant damage can occur if the lamps illuminate a given set of plants for more than a few minutes. It might be possible to reduce the wattage of these lamps or the duration of plant exposures to mitigate against these issues, but the thermal loads from tungsten halogen lamps are very high and may preclude their use in a lunar or martian ALS system in which the power available will be severely limited.

Third, there were significant difficulties encountered with the MCW, HPS, MH, and FL lamps that all centred around increased noise and spectral scatter caused by either the lack of photons in unique spectral regions or high lamp output in specific spectral emission bands. The advantages of these lamps over the tungsten lamps for ALS applications were that they all had lower thermal signatures than the tungsten lamps and that they have been proposed as primary illumination sources for crop production (Wheeler & Martin-Brennan 2000; Wheeler *et al.* 2003). However, based on the current experiments, these lamps do not appear to be able to produce smooth and easily interpretable spectra of plants under stress. Some success was noted for the MCW, HPS, MH, and FL lamps in detecting plant stress related to nutrient levels, chlorophyll concentrations, and leaf areas, but these lamps have other disadvantages that may also preclude their use in ALS modules. The primary disadvantages of the MCW, HPS, MH, and FL lamps for ALS applications were as follows: (a) replacement costs of burned out lamps would raise the ESM of the system; (b) these lamps still had a reasonably high thermal signature that would require additional cooling capacity of the ALS system, which would also raise the ESM; and (c) decreased detection efficiencies for plants under stress caused by the spectral issues discussed above.

Finally, the red/blue LED arrays used here yielded very unusual spectra that were likely fluorescence spectra, and not reflectance spectra. However, the red/blue LED arrays used here were designed for optimum plant growth, and not for optimum remote sensing measurements. The peak bands for chlorophyll absorption of light are in the blue (centred at 460 nm) and in the red (centred at 660 nm) regions (McCree 1972). These were the bands used by the LED arrays, and, thus, it was expected that there would be very little reflectance from plant canopies at these bands.

Based on the above discussion, we propose that the best approach for minimizing the thermal signatures of remote sensing lamps for ALS applications, while also potentially capturing the greatest diversity of remote sensing information, would be to design a LED illumination source with a diversity of LED lamps tailored for optimum remote sensing measurements. Such a LED illumination array could be designed to capture both reflectance and fluorescence data. For example, based on the remote sensing results reported here, LEDs with emissions centred at 550, 685, and higher than 780 nm could be used to generate reflectance algorithms similar to those used here. In order to avoid the fluorescent band at 740 nm induced by excitation by either the 550 or 685 nm LEDs (Fig. 7(b)), near infrared LEDs above 780 nm would be required to measure the NIR reflectance of plant canopies. Past research has clearly shown that NIR bands all the way out to 800 nm can be used effectively for common remote sensing algorithms such as the NIR/green ratio, NIR/red ratio, and NDVI (Buschmann & Nagel 1993; Lichtenthaler 1996). In a preliminary comparison with the current data, the NIR bands at 760 or 780 nm could be used effectively in the reflectance algorithms NIR/R550, NIR/R685, or NDVI to yield very similar results because the NIR bands from 740 to 1350 nm respond in nearly identical ways across the full range (data not shown). Furthermore, the LED

https://doi.org/10.1017/S1473550406003053 Published online by Cambridge University Press

arrays could be designed with individual diodes with emissions at 440 to 470 nm to induce chlorophyll fluorescence at 685 and 740 nm. The maximum excitation wavelengths for inducing chlorophyll fluorescence are 440 and 470 nm (Lichtenthaler *et al*. 1996; Richards *et al*. 2003), and to lesser extents all wavelengths shorter than about 660 nm (Schuerger unpublished). Then the total suite of light-emitting diodes could be wired to permit the operation of individual wavelengths, depending on the remote sensing measurement required. The blue LEDs at either 440 or 470 nm could be operated for optimizing chlorophyll fluorescence, and then shut off for spectral reflectance measurements. The LEDs at 550, 685, and 780 nm could then be switched on to capture key spectral reflectance measurements at bands typically used for reflectance (Buschmann & Nagel 1993; Carter 1993, 1994; Lillesand & Kieffer 1994; Gitelson & Merzlyak 1996, 1997; Lichtenthaler 1996; Schowengerdt 1997; Richards *et al*. 2003).

Finally, LED illumination systems can be designed with a subset of diodes selected to optimize plant growth and development. Recent progress on using LED illumination sources for plant growth under simulated ALS conditions have proven very effective in producing high-quality plant canopies and in reaching acceptable levels of crop productivity (Brown *et al*. 1995; Goins *et al*. 1997; Yorio *et al*. 2001; Kim *et al*. 2004a, b). Based on this literature, a plant growth LED array might require blue (440–460 nm), red (660–685 nm) and near infrared (740–760 nm) light to optimize plant growth and development. In addition, green photons near 550 nm have been shown to increase plant yield (Kim *et al*. 2004a) even though this wavelength is not in the region of maximum absorption for chlorophyll (McCree, 1972). Comparing the optimum wavelengths of visible and near-infrared light required for plant growth and remote sensing measurements indicates that many of the same bands could suffice for both operations. However, a complete plant growth and remote sensing LED array has not yet been described in the literature, but should not be difficult to engineer once the basic requirements are understood for both applications.

Conclusions

Very little work has been published on developing a remote sensing system for detecting plant stresses in future bioregenerative ALS systems. The results of the current study indicated that although the reflectance spectra of tungsten halogen lamps provide the smoothest and most easily interpretable spectra from both healthy and stressed pepper plants, the thermal signatures of the tungsten lamps might preclude their use in plant growing systems deployed for ALS modules. The MCW, HPS, MH, and FL lamps tested here yielded positive results such that they could be used to collect plant stress data for an automatic remote sensing system, but their draw backs included high noise and spectral scatter due to lack of photons in specific regions, higher noise in the VIS and NIR regions due to high spectral emission lines, and moderate to high thermal signatures. Although the red/blue LED arrays used here exhibited low correlations between plant stress biometrics and typical NIR to VIS band ratios or algorithms, they still hold the potential for optimising a diversity of remote sensing measurements while also keeping the thermal signatures and power consumption down within ALS modules. Recall that the LED arrays used herein were not pre-optimized for remote sensing measurements but were instead designed as plant-growth illumination sources. In addition, LED lighting systems can be designed that have separate sets of individually controlled LEDs such that one set can be optimized for plant growth in ALS modules, and a second set of LEDs optimized for remote sensing activities. The different LED sub-systems could be then switched on or off electronically to provide the optimum spectrum for the specific task at hand. Thus, LEDs for remote sensing activities in ALS modules hold the greatest potential to keep the ESM of these systems down by combining plant growth and remote sensing illumination into a single system. New research is underway that will seek to select the optimum suite of LEDs that would combine plant growth and remote sensing capabilities in a single system.

Acknowledgement

This research was supported by the NASA Marshall Flight Center, Space Partnership Development Agreement No. NCC8-221, and by the Life Sciences Support Contract at the Kennedy Space Center, Florida. In addition, we thank personnel at the Boeing Aerospace Company, Electromagnetics Effects Laboratory at the Kennedy Space Center, Florida for their assistance in collecting the radiation output of the seven lamps using the solar panel.

References

Barta, D.J., Tibbitts, T.W., Bula, R.J. & Morrow, R.C. (1992). Evaluation of light emitting diode characteristics for a space-based plant irradiation source. *Adv. Space Res.* **12**, 141–149.

Boston, P.J. (1981). Low-pressure greenhouses and plants for a manned research station on Mars. *J. Br. Interplanet Soc.* **54**, 189–192.

Brown, C.S., Schuerger, A.C. & Sager, J.C. (1995). Growth and photomorphogenesis of pepper plants under red light-emitting diodes with supplemental blue or far-red lighting. *J. Amer. Soc. Hort. Sci.* **120**, 808–813.

Bula, R.J., Morrow, R.C., Tibbitts, T.W., Barta, D.J., Ignatius, R.W. & Martin, T.S. (1991). Light-emitting diodes as a radiation source for plants. *HortScience* **26**, 203–205.

Buschmann, C. & Nagel, E. (1993). In vivo spectroscopy and internal optics of leaves as basis for remote sensing of vegetation. *Int. J. Rem. Sens.* **14**, 711–722.

Carter, G.A. (1993). Responses of leaf spectral reflectance to plant stress. *Am. J. Bot.* **80**, 239–243.

Carter, G.A. (1994). Ratios of leaf reflectance in narrow wavebands as indicators of plant stress. *Int. J. Rem. Sens.* **15**, 697–703.

Drysdale, A.E., Ewert, M.K. & Hanford, A.J. (1999). Equivalent System Mass studies of missions and concepts. *SAE Technical Paper Series 1999-01-2081*. SAE International Publishing, Warrendale, PA.

Eckart, P. (1996). *Spaceflight Life Support and Biospherics*. Kluwer Academic Publishers & Microcosm Press, Dordrect, The Netherlands.

Ewert, M.K., Drysdale, A.E., Hanford, A.J. & Levri, J. (2001). Life Support Equivalent System mass predictions for the Mars dual lander reference mission. *SAE Technical Paper Series 01-2358*. SAE International Publishing, Warrendale, PA, USA.

Ferl, R.J., Schuerger, A.C., Paul, A.-L., Gurley, W.B., Corey, K.A. & Bucklin, R. (2002). Plant adaptation to low atmopsheric pressures: Potential molecular responses. *Life Support & Biosph. Sci.* **8**, 93–101.

Gitelson, A.A. & Merzlyak, M.N. (1996). Signature analysis of leaf reflectance spectra: Algorithm development for remote sensing of chlorophyll. *J. Plant Physiol.* **148**, 494–500.

Gitelson, A.A. & Merzlyak, M.N. (1997). Remote estimation of chlorophyll content in higher plant leaves. *Int. J. Rem. Sens.* **18**, 2691–2697.

Goins, G.D. & Yorio, N.C. (2000). Spinach Growth and Development under Innovative Narrow- and Broad-Spectrum Lighting Sources. *SAE Technical Paper Series 2000-01-2290*. SAE International, Warrendale, PA, USA, p. 8.

Goins, G.D., Yorio, N.C., Sanwo, M.M. & Brown, C.S. (1997). Photomorphogenesis, photosynthesis, and seed yield of wheat plants grown under red light-emitting diodes (LEDs) with and without supplemental blue light. *J. Exp. Bot.* **48**, 1407–1413.

Gonzales, A.A., Schuerger, A.C., Mitchell, R. & Barford, C. (1996). Engineering strategies for the design of plant nutrient delivery systems for use in space: Approaches to countering microbiological contamination. *Adv. Space Res.* **18(4/5)**, 5–20.

Kuhn, W.R. & Atreya, S.K. (1979). Solar radiation incident on the Martian surface. *J. Mol. Evol.* **14**, 57–64.

Kim, H.-H., Goins, G.D., Wheeler, R.M. & Sager, J.C. (2004a). Green-light supplementation for enhanced lettuce growth under red- and blue-light-emitting diodes. *HortScience* **39**, 1617–1622.

Kim, H.-H., Goins, G.D., Wheeler, R.M. & Sager, J.C. (2004b). Stomatal conductance of lettuce grown under or exposed to different light qualities. *Ann. Bot.* **94**, 691–697.

Lichtenthaler, H.K. (1996). *Vegetation Stress*. Gustav Fischer Publishers, New York, p. 649.

Lichtenthaler, H.K., Gitelson, A.A. & Lang, M. (1996). Non-destructive determination of chlorophyll content of leaves of a green and an aurea mutant of tobacco by reflectance measurements. *J. Plant Physiol.* **148**, 483–493.

Lillesand, T.M. & Kiefer, R.W. (1994). Remote Sensing and Image Interpretation. John Wiley & Sons, Inc., New York, p. 750.

McCree, K.J. (1972). The action spectra, absorbtance and quantum yield of photosynthesis in crop plants. *Agric. Meteorol.* **9**, 191–196.

Ming, D.W. & Henninger, D.L. (eds) (1989). *Lunar Base Agriculture: Soils for Plant Growth*. Amer. Soc. Agron. Madison, WI, p. 255.

Norikane, J., Goto, E., Kurata, K. & Takakura, T. (2003). A new relative referencing method for crop monitoring using chlorophyll fluorescence. *Adv. Space Res.* **31**, 245–248.

Olson, R.L., Oleson, M.W. & Slavin, T.J. (1988). CELSS for advanced manned mission. *HortScience* **23**, 275–293.

Omasa, K. (2001). Phytobiological IT in CELSS. In *Advanced Technology of Environment Control and Life Support*, eds Tako, Y., Shinohara, M., Komatsubara, O. & Nitta, K., pp. 244–251. Institute for Environmental Sciences, Tokyo.

Paul, A.-L., Schuerger, A.C., Popp, M.P., Richards, J.T., Manak, M.S. & Ferl, R.J. (2004). Hypobaric biology: Arabidopsis gene expression at low atmospheric pressure. *J. Plant Physiol.* **134**, 215–223.

Richards, J.T., Schuerger, A.C., Capelle, G.A. & Guikema, J.A. (2003). Laser-induced fluorescence spectroscopy of dark- and light-adapted bean (*Phaseolus vulgaris* L.) and wheat (*Triticum aestivum* L.) plants grown under three irradiance levels and subjected to fluctuating lighting conditions. *Rem. Sens. Environ.* **84**, 323–334.

Schowengerdt, R.A. (1997). *Remote Sensing: Models and Methods for Image Processing*. Academic Press, New York, p. 522.

Schuerger, A.C. (1998). Microbial contamination of advanced life support (ALS) systems poses a moderate threat to the long-term stability of space-based bioregenerative systems. *Life Support & Biosph. Sci.* **5**, 325–337.

Schuerger, A.C. (2004). Microbial Ecology of the Surface Exploration of Mars with Human-Operated Vehicles. In *Martian Expedition Planning*, ed. Cockell, C.S. Univelt Publishers, Santa Barbara, CA, American Astronautical Society publication AAS 03-322, pp. 363–386.

Schuerger, A.C. unpublished.

Schuerger, A.C. & Brown, C.S. (1997). Spectral quality affects disease development of three pathogens on hydroponically grown plants. *HortScience* **32**, 96–100.

Schuerger, A.C. & Mitchell, D.J. (1992). Effects of temperature, hydrogen ion concentration, humidity, and light quality on disease severity of *Fusarium solani* f. sp. *phaseoli*. *Can. J. Bot.* **70**, 1798–1808.

Schuerger, A.C., Mancinelli, R.L., Kern, R.G., Rothschild, L.J. & McKay, C.P. (2003). Survival of endospores of *Bacillus subtilis* on spacecraft surfaces under simulated Martian environments: Implications for the forward contamination of Mars. *Icarus* **165**, 253–276.

Schuerger, A.C., Ming, D.W., Newsom, H.E., Ferl, R.J. & McKay, C.P. (2002). Near-term lander experiments for growing plants on Mars: Requirements for information on chemical and physical properties of Mars regolith. *Life Support & Biosph. Sci.* **8**, 137–147.

Schwartzkopf, S.H. (1992). Design of a Controlled Ecological Life Support System. *BioScience* **42**, 526–535.

Tibbits, T.W. & Alford, D.K. (1982). Controlled Ecological Life Support System: Use of Higher Plants. *NASA Conf. Publ.* 2231. NASA Ames Research Center, Moffett Field, CA, p. 81.

Wheeler, R.M. & Martin-Brennan, C. (2000). Mars Greenhouses: Concepts and Challenges. *NASA Technical Memorandum 2000-208577*, Kennedy Space Center, FL, p. 140.

Wheeler, R.M. *et al.* (2003). Crop Production for Advanced Life Support Systems: Observations from the Kennedy Space Center Breadboard Project. *NASA-TM 2003-211184*, Kennedy Space Center, FL, p. 58.

Woodhouse, R., Heeb, M., Berry, W., Hoshizaki, T. & Wood, M. (1994). Analysis of remote reflection spectroscopy to monitor plant health. *Adv. Space Res.* **14**, 199–202.

Yorio, N.C., Goins, G.D., Kagie, H.R., Wheeler, R.M., & Sager, J.C. (2001). Improving spinach, radish, and lettuce growth under red Light-emitting diodes (LEDs) with blue light supplementation. *HortScience* **36**, 380–383.